Pergamon

Geochimica et Cosmochimica Acta, Vol. 67, No. 15, pp. 2793–2803, 2003

0016-7037/03 $30.00 + .00

doi:10.1016/S0016-7037(03)00099-1

Studies of equilibrium, structure, and dynamics in the aqueous Al(III)-oxalate-fluoride system by potentiometry, ^{13}C and ^{19}F NMR spectroscopy

ANDREA BODOR,[1] IMTE TÓTH,[1,*] ISTUDOR BÁNYAI,[2] LÁSZLÓ ZÉKÁNY,[1] and STAFFAN SJÖBERG[3]

[1]Department of Inorganic and Analytical Chemistry, University of Debrecen, H-4010 Debrecen, Pf. 21, Hungary
[2]Department of Physical Chemistry, University of Debrecen, H-4010 Debrecen, Pf. 7, Hungary
[3]Department of Inorganic Chemistry, University of Umeå, S-90 187 Umeå, Sweden

(*Received April* 29, 2002; *accepted in revised form October* 8, 2002)

Abstract—The $AlOx_{1-3}$ (Ox = oxalate) species were identified in 0.6 M aqueous NaCl by ^{13}C nuclear magnetic resonance (NMR). Rate constants and activation parameters for intramolecular *cis*/*trans* isomerization of the Werner-type $AlOx_2^-$ complex ($k(298\ K) = 5\ s^{-1}$, $\Delta H^{\#} = 67 \pm 5\ kJ\ mol^{-1}$, $\Delta S^{\#} = -6 \pm 6\ J\ mol^{-1}\ K^{-1}$, the rate determining step could be the breaking of the Al–O(C=O) bond) and a very slow intermolecular ligand exchange reaction of $AlOx_3^{3-}$ complex and the free ligand ($k_{30}(298\ K) = 6.6 \cdot 10^{-5}\ s^{-1}$, $\Delta H^{\#} = 164 \pm 17\ kJ\ mol^{-1}$, $\Delta S^{\#} = 225 \pm 51\ J\ mol^{-1}\ K^{-1}$, D/I_d mechanism) were determined by dynamic 1D and 2D ^{13}C NMR measurements. Mixed complexes, AlFOx, $AlFOx_2^{2-}$, AlF_2Ox^-, and $AlF_2Ox_2^{3-}$, with overall stability ($\log\beta$) of 11.53 ± 0.03, 15.67 ± 0.03, 15.74 ± 0.02, and 19.10 ± 0.04 were measured by potentiometry using pH- and fluoride-selective electrodes and confirmed by ^{13}C and ^{19}F NMR. The role of these complexes in gibbsite dissolution was modeled. The mixed Al(III)-Ox^{2-}-F^- complexes have to be considered as the chemical speciation of Al(III) in natural waters is discussed. *Copyright © 2003 Elsevier Science Ltd*

1. INTRODUCTION

Aluminum mobility in the environment has attracted considerable attention in recent times because of the acidification of natural waters and soils arising from acid rain (Smith, 1996). The solubility and transport of aluminum is substantially increased by complex formation. As a "hard" metal ion, Al(III) has an affinity for "hard" donors such as O-containing compounds and F^-. These ligands are widely found in geochemical, biologic, and industrial systems.

Oxalate, $C_2O_4^{2-}$ (referred to from now on as Ox^{2-}) is intensively studied from many points of view. It is one of the most abundant low-molecular-weight organic ligands present in organic matter in soils (Smith, 1996). Oxalate is a major metabolic product of fungi in natural environments, and it is highly biodegradable. Material science shows interest in oxalate as a versatile building block for new magnets (Mörtl et al., 2000). Oxalate forms strong complexes with Al(III). In a combined study of e.m.f. with ^{27}Al nuclear magnetic resonance (NMR) (Sjöberg and Öhman 1985), $AlOx_i^{(3-2i)+}$ (i = 1–3) species among polynuclear and mixed hydroxo complexes were detected. ^{27}Al NMR measurements showed octahedral geometry for the $AlOx_i$ species in solution (Phillips et al., 1997b). Several structures have been determined in solid $M_3(AlOx_3) \cdot 3H_2O$ compounds. In all cases aluminum is six coordinated with three bidentate oxalate ligands (Powell and Heath, 1996).

The fluoride complexes of Al(III) have also been studied. The system is deceptively simple in the acidic pH range as it is represented well by the formation of a series of complexes, $AlF_i^{(3-i)+}(aq)$ (i = 1–5) (Bodor et al., 2000; Hefter et al., 2000 and references therein).

Time dependence of the equilibration is a key factor for speciation and can also be important for transport, or dissolution of minerals. Al-complexes are often formed in very slow reactions. Kinetic information evaluated in the homogenous aqueous phase is said to be useful for explaining dissolution mechanism of minerals (Casey and Westrich, 1992). The rate of water exchange for $AlOx(H_2O)_4^+$ and $AlF_i(H_2O)_{6-i}^{(3-i)+}$ (i = 1, 2) species has been studied recently. It is found that the lability of the Al(III)–O bond of coordinated water is substantially increased by coordination of a dicarboxylic chelate, or fluoride(s) in the inner–sphere of the metal ion (Phillips et al., 1997a,b). The slow ligand exchange reaction of $Al(Ox)_3^{3-}$ has been studied with a radiotracer method (Long, 1941). In our recent ^{19}F NMR study we have found that the kinetics in the Al(III)–F^- system is dominated by F^- exchange rather than complex formation, and the *cis/trans* isomerization of $AlF_2^+(aq)$ is slowed sufficiently to be observed at temperatures around 270 K (Bodor et al., 2000).

The aim of this paper is to further characterize the aluminum–oxalato binary species and explore the aluminum–oxalato–fluoro ternary system in solution. Equilibrium, structural and intrinsic dynamic evaluations are based on potentiometric titrations with pH- and fluoride-selective electrodes, and 1D and 2D ^{19}F and ^{13}C-NMR spectroscopy.

2. MATERIAL AND METHODS

2.1. Materials

Aluminum chloride solution was prepared from 99.9999% purity Al wire (Ajka, Hungary) as described elsewhere (Bodor et al., 2000). Sodium fluoride (Merck p.a.) was crystallized from distilled water, dried at 120°C, and kept in a desiccator. Stock solutions of 0.200 mol/L and 0.0500 mol/L NaF were prepared by weight. Sodium chloride, sodium oxalate (with no ^{13}C enrichment for potentiometry), and sodium hydroxide (Merck p.a.) were used without further purification.

NMR samples were prepared by adding calculated volumes of 0.10 mol/L Na_2Ox solution (99% ^{13}C enriched, Cambridge Isotope Laboratories) to $AlCl_3$ stock solution. The NMR samples were prepared 1 day before the NMR measurements, although no time dependence of the spectra was found after a few minutes. The ionic medium was kept

* Author to whom correspondence should be addressed (imretoth@delfin.klte.hu).

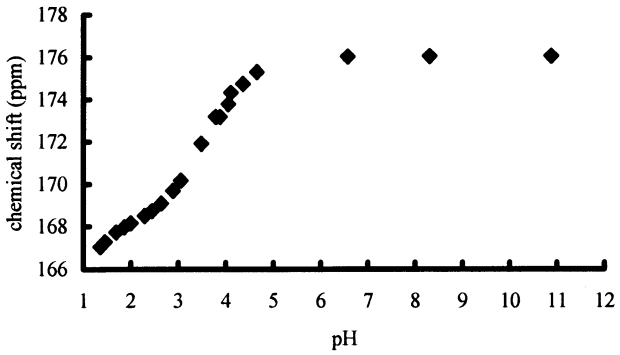

Fig. 1. ^{13}C-NMR shift vs. pH curve of 5 mM Na_2Ox sample in 0.6 mol/L NaCl.

at 0.6 mol/L Na(Cl). 10% D_2O was added for the deuterium lock. The required acid, if needed, was added as HCl. pH measurements for the NMR samples were done with a combined glass-Ag/AgCl electrode (Radiometer GK2401B) or in the case of fluoride containing samples with a HF-resistant combined electrode (Ingold, HF-405-60-57) connected to a Radiometer PHM84 pH-meter and calibrated using the method of Irving et al. (1967). No correction was made for the deuterium isotope effect.

Occasionally the pH had to be measured in samples with little buffer capacity, or in very acidic solutions. In this case, pH was calculated from the total acid concentration, or measured in situ by monitoring the observed time-averaged NMR shift (δ_{obs}) of a properly chosen HL/L$^-$ signal. In our particular case the ^{13}C-NMR signal of the free oxalate ligand was used to follow pH, as the ligand exchange between the free ligand and ML_i was slow on the actual NMR time scale, while the proton exchange for H_iL species was fast. A chemical shift vs. pH curve is shown in Figure 1.

2.2. NMR Measurements

2.2.1. 1D NMR experiments

^{19}F NMR spectra were recorded at 470.5 MHz with Bruker DMX500 and DRX500 spectrometers using a 5-mm inverse probe head in locked mode. The samples were introduced in polytetrafluoroethylene NMR tubes, which were inserted into conventional 5-mm glass tubes. Typical NMR parameters were: flip angle ~30° (6–8 μs), pulse repetition time 0.8–1.5 s, spectral window 4250–11,800 Hz, number of scans 64–160. The chemical shifts are reported in ppm toward lower frequencies with respect to an aqueous alkaline solution of 0.01 mol/L NaF taken δ = 0.00 ppm. In Table 1. we report these chemical shift values relative to the commonly used $CFCl_3$ as well.

^{13}C-NMR spectra were recorded at 90 and 125 MHz with a Bruker AMX360 using a QNP probe head and DMX500 and DRX500 spectrometers using a 5-mm inverse probe head in locked mode. Typical acquisition parameters for ^{13}C-NMR spectra were: flip angle 13 μs (30°), pulse repetition time 15 s, spectral window 3000 Hz, number of scans 32–256. These parameters enabled obtaining quantitative integrations from the spectra recorded on samples containing 99% ^{13}C-enriched oxalate.

The temperature of the probe head was checked by the "methanol-thermometer method" (van Geet, 1970). Spectra were analyzed using the Bruker WIN-NMR software.

Table 1. Overall stability constants of $AlF_pOx_q^{(3-p-2q)+}$ species, $\log\beta_{pq}$, determined in 0.6 M NaCl at 25°C, together with ^{19}F and ^{13}C NMR shifts and number of possible isomers.

Species	$\log\beta_{pq}$ [a]	δ_F (ppm)[b]	δ_F (ppm)[c]	δ_c (ppm)	Possible isomers
AlFOx	11.53 ± 0.03	~−40	−241	168.42	2
AlF_2Ox^-	15.67 ± 0.03	−38.60	−239.60	168.77	4
$AlFOx_2^{2-}$	15.74 ± 0.02	−39.55	−240.55	168.51	2
$AlF_2Ox_2^{3-}$	19.10 ± 0.04	−39.34	−240.34	168.99	2

[a] The uncertainty is equal to three times the estimated standard deviations in the least-squares refinement of the experimental data.
[b] Chemical shift referred to NaF.
[c] Chemical shift referred to $CFCl_3$.

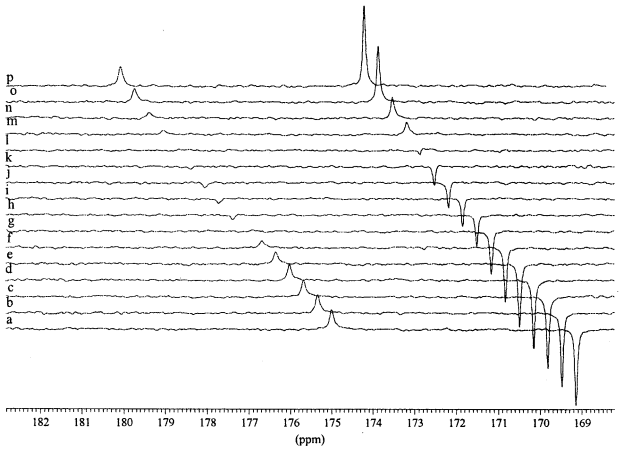

Fig. 2. ^{13}C-NMR (90 MHz) spectra of a solution with c_{Al} = 8 mM, c_{Ox} = 32 mM, pH = 4.02, at 362 K. Corresponding values of the variable delay list are (a) 0.6 ms, (b) 0.01 s, (c) 0.03 s, (d) 0.05 s, (e) 0.1 s, (f) 0.2 s, (g) 0.4 s, (h) 0.8 s, (i) 1.2 s, (j) 1.5 s, (k) 2.5 s, (l) 5.0 s, (m) 8.0 s, (n) 10.0 s, (o) 20.0 s, (p) 30.0 s. The signal of $AlOx_3^{3-}$ is inverted.

2.2.2. Dynamic NMR studies

Both T_2 and T_1 time scales could be used to follow the dynamics in our system. Line width data of signals found in the "slow exchange regime" on the actual chemical shift time scale were evaluated by fitting Lorentz curves. Line broadening (LB in Hz) of the ^{13}C-NMR signals, due to the chemical exchange was calculated as $LB = LW^{obs} - LW^0$, where LW^{obs} was the observed line width, and LW^0 was the nonexchange line width of the signal, respectively. For all exchanging sites in ^{13}C-NMR, $LW^0 \approx 1$ Hz was obtained in independent experiments. The pseudo-first-order rate constants were calculated by using the formula $k^{obs} = LB \cdot \pi$ (Sandström, 1982).

Complete band shapes of ^{13}C-NMR spectra were analyzed by simulation of measured spectra according to Chan and Reeves (1970) using a homemade program written in MATLAB. The measured and calculated spectra were compared with respect to the line widths, relative intensities, and positions of the peaks. The initial input parameters for simulation were the chemical shift values, populations, nonexchange line widths. These data were obtained from the deconvolution of a measured spectrum, being in slow exchange. The simulation is conducted with a rate constant value given in the input, and the goodness of the fitting is accepted, when the line width and intensities of the measured and simulated spectra are the same. This is the reason why there is no error given for the rate constant.

Magnetization transfer experiments, as the one shown in Figure 2, were done in two ways. The outcome is the same, regardless which sequence was applied. The simplest rectangular shaped Dante sequence was used with typically 30–50 pieces 1–1.2 μs long pulses applying ca. 0.5 ms delays in between. The total pulse length and the selectivity were roughly calculated then tuned experimentally, usually achieving 85–95% efficiency for inversion. When studying two signals, magnetization transfer (MT) was made by the method of three hard pulses. The scheme is: $90°_x$–τ_1–$90°_y$–VD–$90°_x$, where the subscripts denote the phase of the exciting pulse. The offset is placed perfectly in the middle of the chemical shifts of the two peaks. $\tau_1 = 1/(4 \cdot \Delta\nu)$, where

$\Delta\nu$ is the difference in chemical shift in Hz. This sequence works as follows: the first pulse creates coherence, rotating the equilibrium magnetization to the y-axis. The transverse magnetization of one of the peaks goes to the x-axis during τ_1, while the other goes to the –x-axis. The peaks are labeled by their chemical shifts. The second 90° pulse rotates the magnetization in $-x$ to $-z$ and that in $+x$ to $+z$. (The selective 180° pulse was composed from two hard 90° pulses similar to the 2D NOESY sequence.) During the variable delay (VD) the longitudinal relaxation and the exchange proceed (mixing time), then the third 90° pulse reads the state of the system. The next transient starts after complete relaxation. The required time was carefully checked experimentally.

The change in magnetization vector (taken from the integrated intensity of the corresponding signal) is given by:

$$\mathbf{M}_t = \exp(\mathbf{R} \cdot t) \cdot (\mathbf{M}_0 - \mathbf{M}_\infty) + \mathbf{M}_\infty$$

where $\mathbf{M}$ is the column matrix of magnetization on each site at time t, $\mathbf{M}_\infty$ is the column matrix of equilibrium longitudinal magnetization. $\mathbf{R}$ is the square rate matrix with off-diagonal elements, $\mathbf{R}_{ij} = k_{ji}$ (the pseudo-first-order rate constant from site j to site i), and diagonal elements, $\mathbf{R}_{ij(i=j)} = -\frac{1}{T_{1i}} - \sum_{i \neq j} k_{ij}$. The unknown parameters $\mathbf{M}_\infty$, T_{1i}, k_{ji} have been fitted with a nonlinear least-squares method using the MATLAB program. In the case of free oxalate, the T_{1i} value has been determined from independent measurements.

^{19}F NMR 2D EXSY spectra were also recorded for the ternary system. The classical NOESY pulse program from Bruker was used

2.3. Potentiometric Titrations

2.3.1. Titration system

The titrations were carried out in a box thermostated at 25°C, using two measuring electrodes. The free H^+ concentration was determined by measuring the e.m.f. of the cell:

$$(-)\ \text{RE} \ //\ \text{equilibrium solution} \ //\ \text{ME}\ (+)$$

where ME was the measuring electrode and RE was the reference electrode. The ME electrode was formed from quinhydrone crystals (recrystallized from water at 70°C) and a Pt foil electrode, which was washed in hot aqua regia and water, then dried in an ethanol flame before each titration. The quinhydrone electrode was used to avoid problems with the glass electrode in connection with fluoride solutions. There was no indication that quinones formed any complexes with Al(III).

The RE was

$$\text{Ag, AgCl/0.01 M } Cl^-, \text{ 0.59 M } ClO_4^- // \text{ 0.6 M NaCl}$$

Free F^- concentration was determined using the following cell:

$$(-)\ \text{RE} \ //\ \text{equilibrium solution} \ //\ \text{ME}'(+),$$

where ME′ was a F^- selective electrode (Metrohm 6.0502.150) and RE was the reference electrode described before. As both electrodes were calibrated on concentration scales in H^+ and F^-, pH and pF correspond to $-\log[H^+]$ and $-\log[F^-]$, respectively.

Titrations were done in a Teflon vessel under N_2 atmosphere. Occasional impurities in the N_2 gas were eliminated by passing the gas through three washing solutions: 10% NaOH, 10% H_2SO_4, and 0.6 mol/L NaCl, and a G_4 filter, respectively.

The maximum equilibration time was set to be 90 min. In general, equilibrium was established in 5 min.

2.3.2. Calibration of the electrodes

E_0 of the electrodes were calculated using the Gran method (Gran, 1952). The Nernst equation for E_0^H was used as follows:

$$E = E_0^H + g \cdot \lg[H^+] + E_j \text{ with } g = 59.16 \text{ mV}$$

Here E_j denotes the liquid junction. As the measurements were made with pH $\geq$2.2, liquid junction effects could be neglected. For E_0^F analogous calculations were performed. In this case the Nernst equation was: $E = E_0^F - g \cdot \lg[F^-] + E_j$

2.3.3. Titration of the Aluminum–Fluoride–Oxalate System

Two possibilities were considered: to prepare first the binary Al–fluoride species and to titrate this solution with oxalate, or to form first the Al–oxalate complexes followed by titration with fluoride. Both ways were checked with the following technical arrangements:

i) titration of $AlF_p^{(3-p)}$ complexes with Ox^{2-} was realized in three steps:
   a) first E_0^H was determined by titrating the 0.6 M NaCl solution with HCl.
   b) the final solution from a) was titrated further with NaF to determine E_0^F.
   c) the necessary amount of $AlCl_3$ was added to the solution from b). After waiting 1 h for equilibration, the solution was titrated with a mixture of $AlCl_3$ and NaF from one burette; thus keeping the c_{Al} and c_F constant; and with a buffer of HOx^-/Ox^{2-} (pH $\cong$ 4) from another burette.

ii) titrations of $AlOx_q^{(3-2q)}$ species with F^- were performed in two steps:
   a) first E_0^H was determined as in *i*).
   b) $AlCl_3$ and a buffer of HOx^-/Ox^{2-} (pH $\cong$ 4) were added to solution a), then titration was done using a burette with a mixture of Al(III) and Ox^{2-} and another burette with a solution of NaF. In this case E_0^F was determined independently via titration of a NaCl solution with NaF before and after each titration.

The equilibrium analysis of experimental potentiometric data was performed by using the computer program LETAGROP VRID (Sillén and Warnquist, 1968). In the calculations of the protonation constants of fluoride and oxalate, the stability constants of aluminum hydroxo species, binary fluoride and oxalate complexes were accounted for (Table 2). Distribution diagrams were calculated by the MEDUSA program (Puigdomenech, 1997) or by the SOLGASWATER program (Eriksson, 1979)

3. RESULTS

3.1. Al(III)–Ox^{2-}–H^+ System

Three binary species, $AlOx^+$, $AlOx_2^-$, and $AlOx_3^{3-}$, are detected in the acidic region, and two polynuclear hydroxo species are also found in the near neutral or slightly alkaline solutions. At our experimental conditions, i.e., at lower pH or at larger excess of oxalate, only binary species are formed up to pH $\leq$ 6.5 (Fig. 3a,b).

3.1.1. Assignment of ^{13}C-NMR Signals of $Al(Ox)_i^{+3-2i}$ species

Dependence of the ^{13}C signal on pH of a 5 mM Ox^{2-} sample in 0.6 mol/L NaCl/HCl is shown in Figure 1. The δ–pH curve for the time-averaged signal of the protonated oxalate ligand begins at pH = 1.36 and comes to the limiting shift of Ox^{2-} at pH $\sim$ 6. The value for the first protonation constant is evaluated from these data by least-squares fitting. $\log\beta_{HOx} = 3.60 \pm 0.03$ is in excellent agreement with the literature value (Sjöberg and Öhman, 1985), whereas the second protonation constant cannot be determined from this pH range. It is worth calling attention to a peculiarity of this pH titration, namely, that the ^{13}C line width of the oxalate signal is substantially broader (5–8 Hz) than the usual width of either the carbonyl carbon peaks, or those of binary species ($\sim$ 0.6 Hz). This broadening is pH dependent, but the variation is not monotonic. Explanation of

Table 2. Composition matrix and formation constants used in the different model calculations.

Complex	Stability constant	H^+	F^-	Ox^{2-}	Al^{3+}	Ref.
HF	2.67	1	1	0	0	1
HF_2^-	3.50	1	2	0	0	1
$Al(OH)^{2+}$	−5.52	−1	0	0	1	2
$Al(OH)_2^+$	−10.31	−2	0	0	1	3*
$Al(OH)_3$	−16.08	−3	0	0	1	3*
$Al(OH)_4^-$	−23.46	−4	0	0	1	2
$Al_3(OH)_4^{5+}$	−13.57	−4	0	0	3	2
$Al_{13}(OH)_{32}^{7+}$	−109.2	−32	0	0	13	2
AlF^{2+}	6.42	0	1	0	1	4
AlF_2^+	11.82	0	2	0	1	4
AlF_3	15.81	0	3	0	1	4
AlF_4^-	18.31	0	4	0	1	4
$Al(OH)F^+$	0.1	−1	1	0	1	5*
$Al(OH)_2F$	−6.40	−2	1	0	1	5*
$Al(OH)_3F^-$	−12.53	−3	1	0	1	5*
$Al(OH)F_2$	4.04	−1	1	0	2	5*
$Al(OH)_2F_{2-}$	−2.41	−2	1	0	2	5*
$Al(OH)F_{3-}$	7.55	−1	1	0	3	5*
HOx^-	3.569	1	0	1	0	2
H_2Ox	4.539	2	0	1	0	2
$AlOx^+$	5.969	0	0	1	1	2
$Al(Ox)_2^-$	10.93	0	0	2	1	2
$Al(Ox)_3^{3-}$	14.88	0	0	3	1	2
$Al_3(OH)_3(Ox)_3$	9.340	−3	0	3	3	2
$Al_2(OH)_2(Ox)_4^{4-}$	13.54	−2	0	4	2	2
$HAlOx^{2+}$	5.94	1	0	1	1	2
AlFOx	11.53	0	1	1	1	6
AlF_2Ox^-	15.67	0	2	1	1	6
$AlFOx_2^{2-}$	15.74	0	1	2	1	6
$AlF_2(Ox)_2^{3-}$	19.09	0	2	2	1	6
$Al(OH)_3(c)$	−9.58	−3	0	0	1	3*

1 (Hefter et al., 2000); 2 (Sjöberg and Öhman, 1985); 3 (Baes and Mesmer, 1976); 4 (Bodor et al., 2000); 5 (Sanjuan and Michard, 1987); 6 This work.

* See text (section 4.3) for explanation of asterisk.

this finding requires systematic study. We believe it is an interesting proton exchange reaction related to H-bonding between the two carboxylate groups of oxalate.

Table 3. ^{13}C NMR shift values of the detected binary species.

Species	Chemical shift (ppm)
$AlOx^+$	168.04
trans-$AlOx_2^-$	168.10
cis-$AlOx_2^-$	168.16
$AlOx_3^{3-}$	168.26

The assignment of ^{13}C-NMR signals in the Al(III)–Ox^{2-}–H^+ system can be done by varying the metal/ligand ratio and pH. The results are summarized in Table 3. The signal intensities follow the calculated distribution, and the assignment of $AlOx^+$ (168.04 ppm) and $AlOx_3^{3-}$ (168.26 ppm) is obvious. Moreover, for the species $AlOx_2^-$, two somewhat broadened signals are detected with equal intensities (Fig. 4). The most

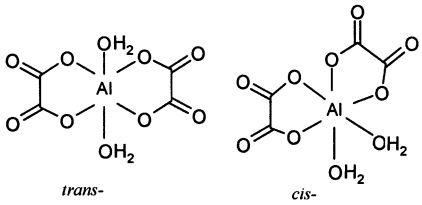

probable explanation for this observation is the existence of two isomers, such as:

It is not possible to decide unequivocally which signal belongs to which isomer. Based on the closer structural similarity of $AlOx_3^{3-}$ to *cis*-$AlOx_2^-$ than to *trans*-$AlOx_2^-$, we tentatively assign the signal at 168.16 ppm to the *cis*-isomer, and the signal at 186.10 ppm to the *trans*-$AlOx_2^-$.

3.1.2. ^{13}C-NMR Dynamics of $Al(Ox)_i^{(3-2i)+}$ Species

Observing two peaks for $AlOx_2^-$ means that the *cis* and *trans* forms are in slow exchange at room temperature. To

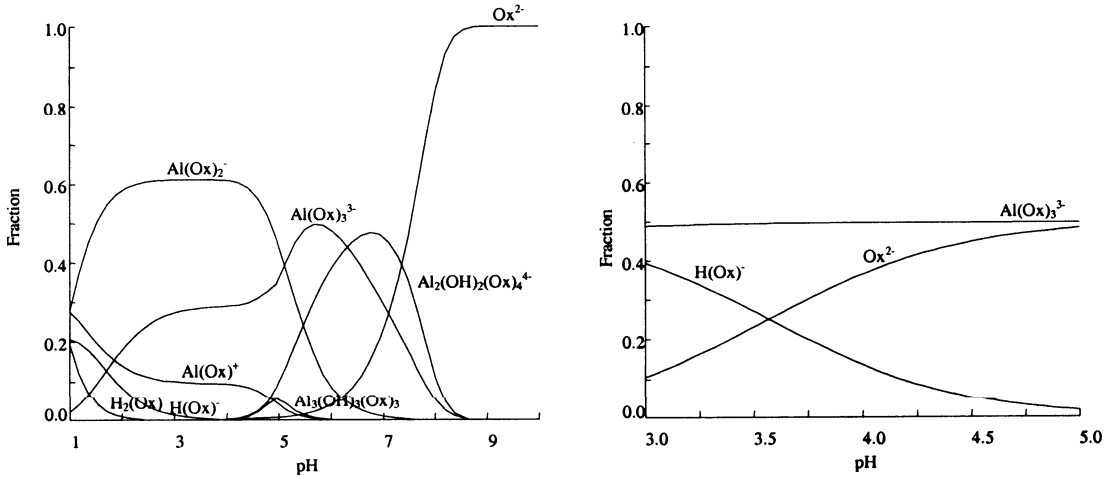

Fig. 3. Distribution diagram as a function of pH (shown for oxalate fraction) for (a) c_{Al} = 5 mM, c_{Ox} = 10 mM, and (b) c_{Al} = 8 mM, c_{Ox} = 48 mM solutions. Arrows indicate the binary species.

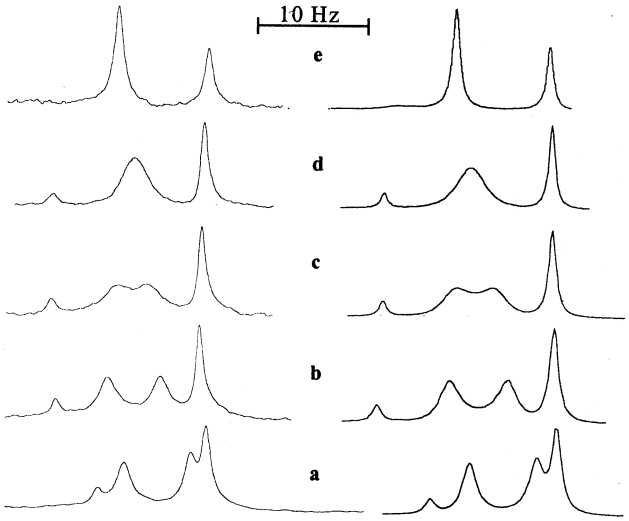

Fig. 4. Measured (left) and simulated (right) ^{13}C-NMR (90 MHz) spectra of a solution with $c_{Al} = 5$ mM, $c_{Ox} = 10$ mM at pH = 2.02 at different temperatures: (a) 278 K, (b) 296 K, (c) 306 K, (d) 315 K, (e) 348 K.

evaluate this intramolecular exchange, a temperature variation study has been done.

The series of spectra (Fig. 4, left) is obtained in a sample having $c_{Al} = 5.0$ mM, $c_{Ox} = 10$ mM, pH = 2.02. $AlOx_2^-$ is the dominant species, followed by $AlOx^+$ and a small portion of $AlOx_3^{3-}$. The free ligand is also present as HOx^- (see Fig. 3a), but its signal is below the detection limit. If it had appeared, it should have coincided with the signals of the binary species. The series of spectra is simulated by a MATLAB microprogram (Fig. 4, right), and the corresponding pseudo-first-order rate constants are calculated (Bányai et al., 2001). The species $AlOx^+$, *cis*-$AlOx_2^-$, *trans*-$AlOx_2^-$, and $AlOx_3^{3-}$ are symbolized as 1, 2, 3, and 4, respectively. The pseudo-first-order intramolecular rate constant is k_{23}. Intermolecular exchange reactions are supposed to occur between the first and second complex, and the second and third one with constants, k_{12}, k_{13}, k_{34}, k_{24}, respectively. Both *cis*- and *trans*- forms of $AlOx_2^-$ are considered to take part with an equal contribution to the exchange reactions. It is almost impossible that a reaction between the first and third complex exists, thus, this exchange is excluded. The goodness of fit for the simulated spectra is reflected by the coincidence of signal intensities and line width values. The individual chemical shifts are calculated from the linear extrapolation of the shifts obtained at lower temperatures. The population of the different sites is given from the deconvolution of signals recorded at 296 K, which coincides with the calculated concentration distribution, and it has been kept constant for all other temperatures. Populations of *cis*- and *trans*-forms of $AlOx_2^-$ are set equal. The fitted pseudo-first-order rate constants are summarized in Table 4.

It can be recognized at first glance of the measured spectra, that the changes in the line shape are related mainly to the signals of the isomers. The important message of this finding is that the isomerization is a two-site exchange, neither the $AlOx^+$ nor the $AlOx_3^{3-}$ are involved in the process, therefore the transformation of the *cis*- to the *trans*-isomer and vice versa

Table 4. Pseudo-first-order rate constants[a] for intramolecular isomerization (k_{23}) of $AlOx_2^-$ and intermolecular ligand exchanges (k_{12}, k_{13}, k_{24}, k_{24}) between binary species.

T (K)	k_{23} (s^{-1})	k_{12} (s^{-1})	k_{13} (s^{-1})	k_{24} (s^{-1})	k_{34} (s^{-1})
278	1.5	–	–	–	–
290	3	–	–	–	–
296	4	–	–	–	–
306	9	–	–	–	–
311	13	–	–	–	–
315	20	–	–	–	–
323	60	0.3	0.3	0.4	0.4
338	$1.5 \cdot 10^2$	0.5	0.5	1	1
348	$1.0 \cdot 10^3$	1.5	1.5	2	2

[a] Notice 1 or 2 significant figures indicating quite large relative uncertainties (20–60%), especially for the slow intermolecular reactions.

should be an intramolecular reaction. At temperatures higher than 306 K, a coalescent peak for the $AlOx_2^-$ species appears in the measured spectra. However, some intermolecular processes are also detected on the T_2 time scale at higher temperatures. Slight broadening of the minor signals appears only in the top trace at $T \geq 323$ K (see Table 4), but this method cannot give quantitative constants for such slow processes. (Observed LB~0.3–1 Hz is close to the detection limit, $k_{obs} = 1\ s^{-1}$ is attributed to $LB = 1/\pi = 0.3$ Hz.) Therefore, magnetization transfer experiments (a typical one is shown in Fig. 2) have been carried out at different temperatures in a sample (with $c_{Al} = 8$ mM, $c_{Ox} = 32$ mM at pH = 4.05). At this pH, only two

$$AlOx_3^{3-} + {}^*Ox^{2-} \underset{k_{0,3}}{\overset{k_{3,0}}{\rightleftharpoons}} Al{}^*OxOx_2^{3-} + Ox^{2-} \qquad (1)$$

signals appear in ^{13}C-NMR, a narrow one for $AlOx_3^{3-}$ (not involved in intramolecular exchange) and a broader one for HOx^-/Ox^{2-}. The exchange reaction between $AlOx_3^{3-}$ and free oxalate is:

Ligand exchange has been detected only at $T \geq 324$ K. Series of spectra have been recorded at higher temperatures, and the evaluated pseudo-first-order intermolecular rate constant values, $k_{30}^{obs}(s^{-1})$ with the temperature values in parentheses (T/K) are: 0.010 ± 0.002 (324); 0.11 ± 0.03 (333); 1.6 ± 0.3 (348); and 6.8 ± 1.7 (362).

3.2. Al(III)–Ox^{2-}–F^-–H^+ System

3.2.1. Potentiometric Study of Speciation and Equilibria

Besides potentiometric measurements, supporting information for the equilibrium model is provided by ^{19}F and ^{13}C-NMR studies. Potentiometric titrations have been carried out to characterize the possible formation of mixed Al(III)–F^-–Ox^{2-} complexes. The overall stability constant, $\beta_{r,p,q}$, is defined according to the general equilibrium:

$$rAl^{3+} + pF^- + qOx^{2-} \rightleftharpoons Al_rF_pOx_q^{(3r-p-2q)+} \qquad (2)$$

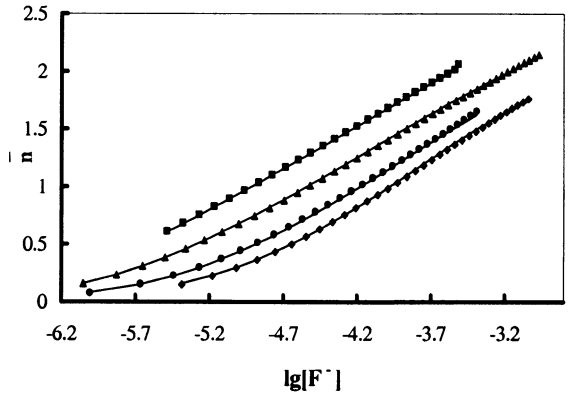

Fig. 5. The average number of coordinated fluoride as a function of free fluoride concentrations at different Al(III):Ox^{2-} ratios. c_{Al} = 5 mM, pH = 2.2–2.7, 0.6 mol/L NaCl at 25°C, c_{Ox} varies: (■) 5 mM, (▲) 8 mM, (●) 12 mM, (♦) 15 mM.

$$\beta_{r,p,q} = \frac{[Al_rF_pOx_q^{(3r-p-2q)+}]}{[Al^{3+}]^r[F^-]^p[Ox^{2-}]^q} \quad (3)$$

Titrations of the binary aluminum–fluoride system with oxalate were described in the experimental part. Titration possibility *i*) failed, in agreement with observations in the Al^{3+}–F^- system (Bodor et al., 2000). Precipitation occurred at ratio c_F: $c_{Al} \geq 2.7$–3 and equilibrium potentials were not reached even in 16 h. Therefore, from the mentioned titration methods at the experimental part, the presented type *ii*) titrations were carried out, i.e., the $Al(Ox)_q$ binary complexes, formed at constant c_{Al} concentration with different excesses of oxalate, were titrated with fluoride. Only a slight variation in pH, between 2.2 and 2.7 was observed. Titration data (Fig. 5) covered the range of $c_F/c_{Al} \leq 3$.

In this figure, experimental data are visualized by plotting the variation of the average number of coordinated fluoride ligands, $\bar{n}_F$, against the logarithm of the free ligand concentration. The $\bar{n}_F$, values for the measured points are calculated with expression (4) resulting from the mass balance equation:

$$c_F = [F^-] + [HF] + 2\cdot[HF_2] + \sum_{p=1}^{5} p\cdot[AlF_p^{(3-p)}] + \sum_{p,q=1}^{4.2} p\cdot[AlF_pOx_q^{(3-2q-p)}] \quad (4)$$

$$\bar{n} = \frac{c_F - [F^-]\cdot\{1 + K_{HF}[H^+] + 2K_{HF_2}K_{HF}[H^+][F^-]\}}{c_{Al}} \quad (5)$$

From Figure 5 it is clear that mixed Al(III)–F^-–Ox^{2-} complexes and/or binary Al(III)–F^- complexes are formed with $p \leq 3$. If we consider six coordinated aluminum ions, then $AlF_pOx^{(1-p)+}$ species with p = 1–3 and $AlF_pOx_2^{(-1-p)}$ with p = 1–2 should form. Due to relatively acidic conditions, mixed hydroxo species, $AlF_pOx_q(OH)_n^{(3-p-2q-n)+}$, are not taken into consideration. Moreover, there is no indication of the formation of protonated and polynuclear species in the working domain in LETAGROP refinements. Keeping the stability constants of binary species fixed and refining those for ternary ones, four complexes are enough and sufficient to describe the system: AlFOx, $AlFOx_2^{2-}$, AlF_2Ox^-, and $AlF_2Ox_2^{3-}$. Refined stability constants are shown in Table 1. and as can be seen from Figure 5 the fit to experimental data is very good. Formation of complexes with higher fluoride content cannot be excluded in more concentrated fluoride solutions or in the presence of other, probably larger, counter cations. These cations may prevent precipitation, as has been detected in the binary aluminum-fluoride system (Brosset and Orring, 1943). However, under our experimental conditions only these four ternary species are present. Formation of other species in solution might be restricted by solubility factors.

3.2.2. ^{13}C and ^{19}F NMR Spectra of Ternary Species

Although NMR spectroscopy does not usually have the precision of potentiometric equilibrium measurements, it can provide an important independent check on their accuracy. Furthermore, analysis of NMR spectra brings us closer to the structural and dynamic features of the species identified by titrations. We have two useful NMR nuclei in the complexes (^{13}C and ^{19}F), and in both cases all four of the ternary species can be found. Assignment has been done by concentration variation measurements. In ^{19}F NMR the situation is easier, as the signals of binary and ternary species are distanced (see Fig. 6b). At the same time the signal of AlFOx is broadened to baseline at 298 K. The ^{13}C-NMR signals overlap. The assignment is also complicated by the presence of free oxalate, which has a substantial shift with small variations in pH. Knowing the positions of binary species and the free oxalate, all peaks can finally be identified. It is also evident that the ternary species do not indicate protonation effects. This is underlined in ^{13}C spectra (Fig. 7), where vertical lines illustrate the invariance of the ternary peak positions with pH changes. On the other hand, the binary $AlOx_2^-$ shows two peaks (*cis*/*trans*), while each of the $AlFOx_2^{2-}$ and $AlF_2Ox_2^{3-}$ species present only one broad peak. This means that oxalate is more labile to isomerization in mixed complexes than in binary ones. Chemical shift values for the four ternary complexes are presented in Table 1.

A striking characteristic of these spectra (Figs. 6 and 7) is that all of the ternary species have broad signals. This may not be surprising if we count the possible Werner type isomers, which are not distinguished by potentiometry, but may be detected in NMR. In a recent study (Martinez et al., 1999) several isomers have been identified in the Al(III)–pyrophosphate–F^- system by ^{31}P and ^{19}F NMR. The temperature variation ^{19}F NMR study (Fig. 8a) shows peculiarities. Three of our four signals, **2**, **3**, and **4** seem to narrow with increasing temperature, indicating that isomers of these complexes are in the "fast exchange regime" on the actual NMR time scale. This must be the consequence of intramolecular isomerization reactions, as we detect as many peaks as the number of species found by independent methods. The number of possible isomers is indicated in Table 1. Lowering the temperature, the AlFOx peak, **1,** narrows while the signal of $AlF_2Ox_2^-$ broadens. This behavior might be an overall effect of complicated inter- and intramolecular exchange reactions. Unfortunately, these exchange reactions could not be separated by temperature variation in the ternary system, in contrast to the binary aluminum–

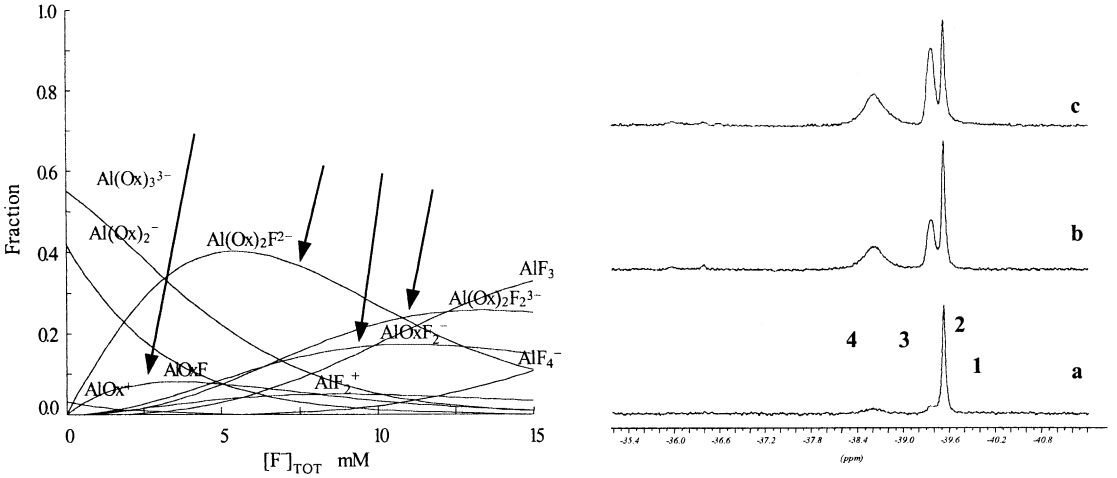

Fig. 6. a) Concentration distribution (Al fraction) of a solution with c_{Al} = 5 mM, c_{Ox} = 15 mM, pH = 2.4 in 0.6 mol/L NaCl media at 298 K. Arrows point out the four ternary species; *b)* ^{19}F NMR (470 MHz) spectra of a solution with composition defined at *a)* at 298 K with varying c_F: (a) 3 mM, (b) 7 mM, (c) 9 mM. Numbers 1, 2, 3, 4 mean complexes AlFOx, $AlFOx_2^{2-}$, $AlF_2Ox_2^{3-}$, and AlF_2Ox^-, respectively. Peak 1 is broadened, see text.

fluoride complexes. Therefore, direct detection of the isomers failed.

To gain further insight into the exchange system, ^{19}F NMR 2D EXSY spectra have been recorded. Off diagonal peaks of Figure 8b indicate exchange between AlF_2^+ and AlF_3; AlF_2^+, AlF_3 and AlF_2Ox^- (4); $AlF_2Ox_2^{3-}$ (3) and AlF_2Ox^- (4), respectively.

4. DISCUSSION

Structural and kinetic studies of the Al(III)–Ox system date back to the birth of coordination chemistry. In this way, the preparation of the optical isomers for the $AlOx_3^{3-}$ complex was attempted in the first half of the last century, conducted similarly as the classical Werner studies. The study of Long using the isotope labeling method clearly proved that this Al(III)-complex was not inert enough for resolvation. At this point it is worthwhile to mention that the term "inert" was not in use when Long's paper was written; it was introduced only in 1952 by Taube (1952).

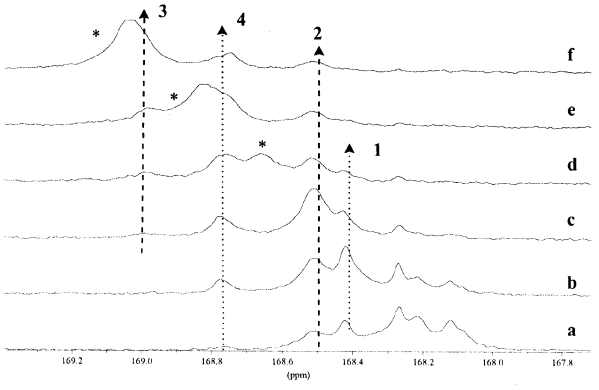

Fig. 7. ^{13}C-NMR spectra (99% enriched ^{13}C, 125 MHz) of a sample with c_{Al} = 5 mM, c_{Ox} = 7 mM, c_H = 7.2 mM, pH = 2.2–2.7 with varying fluoride concentration c_F: (a) 2.5 mM, (b) 5.0 mM, (c) 7.5 mM, (d) 10.0 mM, (11) 12.5 mM, (e) 15.0 mM. Numbers 1, 2, 3, 4 mean complexes AlFOx, $AlFOx_2^{2-}$, $AlF_2Ox_2^{3-}$, and AlF_2Ox^-, respectively.* stays for HOx^-/Ox^{2-}, binary $AlOx_i^{(3-2i)+}$ species are not numbered.

4.1. Structure of $AlOx_2^-$

Existence of two signals for $AlOx_2^-$ with equal intensities is direct proof for *cis/trans* isomers. The equal population is valid for quite a broad temperature range, indicating very close energies of the two structures, contrary to the equivalent isomers of AlF_2^+ complexes. To the best of our knowledge there are no isomers of $AlOx_i$ species characterized in the literature. It is worth mentioning that all signals are very close to each other on the ^{13}C-NMR chemical shift scale. At 90 MHz the chemical shift difference e.g., for $AlOx^+$ and (one of the) $AlOx_2^-$ is 0.06 ppm = 5.4 Hz. Consequently, at the lower field used in an earlier study, only the time-averaged, somewhat broadened signal of the two $AlOx_2$ isomers could be detected (Jaber et al., 1977). However apart from the Werner type inert Co(III) and Cr(III) complexes, this kind of isomers has recently been detected by NMR for the vanadyl(V)–oxalate (Ehde et al., 1991) and uranyl(VI)–oxalate systems (Szabó and Grenthe, 1998).

4.2. Mechanism of Oxalate Exchange Reactions

4.2.1. Cis/trans Isomerization of $AlOx_2^-$

The intramolecular exchange measurements cover a temperature range of 70 K for $AlOx_2^-$, as seen from Table 4. Thus, reliable activation parameters can be calculated. The following data are obtained from the Eyring plot: $\Delta H^{\#} = 67 \pm 5$ kJ mol^{-1}, $\Delta S^{\#} = -6 \pm 6$ J mol^{-1} K^{-1}. These values are in the usual range considering fluxional processes with pure intramolecular character. For these processes the activation entropy values are around zero. The calculation of $\Delta G^{\#}_{298}$ = 69 kJ

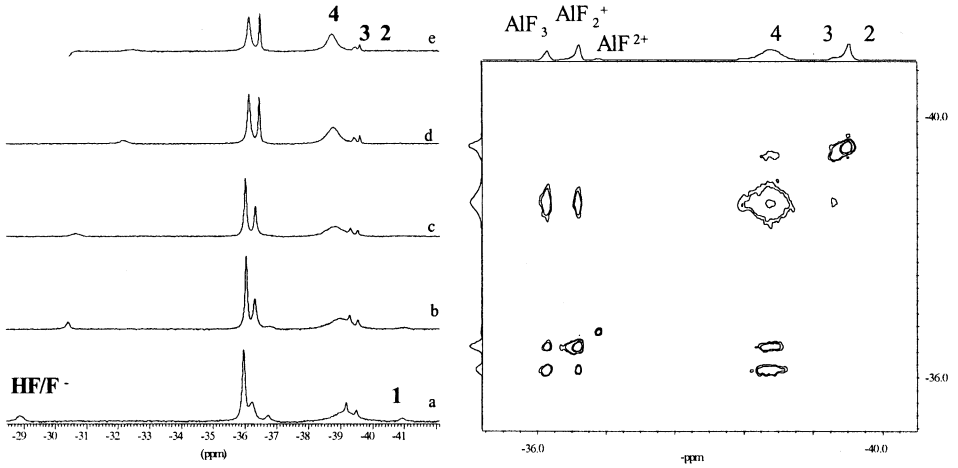

Fig. 8. *a)* ^{19}F NMR (470 MHz) spectra of a solution with $c_{Al} = c_{Ox} = 5$ mM, $c_F = 7$ mM, pH = 2.2 in 0.6 mol/L NaCl media at varying temperatures: (a) 278 K, (b) 238 K, (c) 288 K, (d) 293 K, (e) 298 K. *b)* 2D EXSY ^{19}F NMR spectra for a sample with $c_{Al} = 5$ mM, $c_{Ox} = 6$ mM, $c_F = 8$ mM, pH = 2.4 in 0.6 mol/L NaCl media at 298 K. Mixing time is 300 ms. Numbers 1, 2, 3, 4 refer to species AlFOx, $AlFOx_2^{2-}$, $AlF_2Ox_2^{3-}$, and AlF_2Ox^-, respectively. Binary complexes and HF/F^- are also indicated.

mol^{-1} for this *cis/trans* rearrangement is more characteristic. This value is around the middle of the interval for these rearrangements given in the literature (Orrel et al., 1990). The *cis/trans* exchange requires mutual exchange of one water molecule and one carboxylate group of the oxalate ligand inside the inner coordination sphere of Al(III), while the other carboxylate could be bound during isomerization. The lability of water ($k_{H_2O} = 109\ s^{-1}$) in $AlOx(H_2O)_4^+$ (and consequently probably in $AlOx_2(H_2O)_2^-$) is said to be much higher (Phillips et al., 1997a) than the rate of the isomerization ($k_{cis/trans}^{298} = 5\ s^{-1}$). Therefore, the rate-determining step should be the breaking of the Al–O(C=O) bond.

4.2.2. Intermolecular Ligand Exchange Reactions

As discussed above, the *cis/trans* isomerization of $AlOx_2^-$ can be described without any contribution from intermolecular reactions. This indicates that bimolecular reactions like complex formation, e.g., $AlOx^+ + Ox^{2-} \rightleftharpoons AlOx_2^-$, are quite slow on the ^{13}C-NMR time scale at room temperature. However, alike the Al^{3+}–F^- system, one can expect ligand exchange reactions, e.g., $AlOx^+ + {}^*Ox \rightleftharpoons Al{}^*Ox^+ + Ox$, (Ox = H_2Ox, HOx^-, Ox^{2-}) to be much faster. Both kinds of reaction require some free oxalate in the equilibrium system and this condition is fulfilled for solutions with $c_{Ox}/c_{Al} > 3$ (and low pH for complexes other than $AlOx_3^{3-}$). All our attempts to detect any exchange between complexes $AlOx_q^{(3-2q)+}$ and free Ox (in pH = 1–4 range and c_{Ox}/c_{Al} = 3–6) using T_1 time scale of ^{13}C-NMR at room temperature failed. In this way, a limiting value $\tau > 3$–5 $T_1 \sim 120$ s ($k_{obs} \sim 1/\tau < 0.008\ s^{-1}$) can be calculated. This limit already shows how inert the 5-membered AlOx ring is to *inter*molecular exchange even in 0.1 mol/L HCl.

However, measurable ligand exchange between $AlOx_3^{3-}$ and free Ox can be detected at higher temperatures. Remembering the lack of bimolecular reactions at room temperature and the minor contributions of intermolecular exchange to the line broadening at higher temperatures (see Fig. 4 and Table 4), this pseudo-first-order rate constant, k_{30}^{obs} (s^{-1}), can be considered as a real first-order constant, $k_{30}(s^{-1})$. A bimolecular reaction between $AlOx_3^{3-}$ and free Ox, e.g., $AlOx_3^{3-} + {}^*Ox^{2-} \rightleftharpoons AlOx_2{}^*Ox^{3-} + Ox^{2-}$ with a second-order rate constant, k_{30} ($M^{-1}s^{-1}$) is very unlikely, because of the saturated coordination sphere of the Al(III) and the unfavorable charges (–3 and –2) of the reactants.

Calculated activation parameters, together with selected literature values are summarized in Table 5. The values of $\Delta H^{\#} = 164 \pm 17$ kJ mol^{-1}, $\Delta S^{\#} = 225 \pm 51$ J mol^{-1} K^{-1} are in accordance with a pure D, or I_d mechanism:

$$AlOx_3^{3-} \xrightarrow{\text{r.d.s.}} AlOx_2^{-\#} + Ox^{2-} \qquad (6)$$

$$AlOx_2^{-\#} + {}^*Ox^{2-} \overset{\text{fast}}{\rightleftharpoons} AlOx_2{}^*Ox \qquad (7)$$

The dissociation of one oxalate occurs in the first slow step, while in the next fast step a new oxalate ligand jumps into the vacancy. The high value of $\Delta H^{\#}$ supports this dissociative rate-determining step (r.d.s.), as two bonds have to be broken. The activated complex will be more disordered, in agreement with the positive value of $\Delta S^{\#}$. The same mechanism is proposed by Ehde et al. (1991) for the fully saturated $VO_2(Ox)_2^{3-}$.

The slow rate of the intermolecular ligand exchange reaction for $AlOx_3^{3-}$, $k_{30} = 6.6 \cdot 10^{-5}\ s^{-1}$, is in apparent contradiction with the unsuccessful experiments to resolve optical isomers of this complex (Long, 1941). An obvious solution for this dilemma, if we assume a similar intramolecular isomerization for $AlOx_3^{3-}$ as we detected for the cis/trans isomerization of $AlOx_2^-$. It could require breaking one Al–O(C=O)–bond for two oxalates, while the opposite ends of the ligands could remain bonded. This bond breaking mechanism could result in a rela-

Table 5. Kinetic parameters of exchange reactions measured in this work together with selected literature values.

Complex/type of exchange reaction	Solvent	$\Delta H^{\#}$ (kJ mol^{-1})	$\Delta S^{\#}$ (J mol^{-1} K^{-1})	k_{298} (s^{-1})	Mechanism	Reference
$AlOx_2^{2-}$/intra-m.isomerisation	water	67 ± 5	−6 ± 6	5 ± 0.5	bond-rupture	this work
$AlOx_3^{3-}$/Oxinter-m.exchange	water	164 ± 17	225 ± 51	$6.6 \cdot 10^{-5}$	D/I_d	this work
$Al(H_2O)_6^{3+}$/water exchange	water	85	42	1.29	D/I_d	1
$AlOx(H_2O)_4^{+}$/water exchange	water	68.9	25.3	109	I_d?	1
$AlF(H_2O)_5^{2+}$/water exchange	water	79	60	$1.11 \cdot 10^{2}$	I_d?	3
$AlF_2(H_2O)_4^{+}$/water exchange	water	69	70	$2.0 \cdot 10^{4}$	I_d?	3
AlF^{2+}/F^- inter-m. ligand exchange	water	–	–	$<2 \cdot 10^{3}$	I_a	4
AlF_2^{+}/F^- inter-m. ligand exchange	water	–	–	$1.5 \cdot 10^{6}$	I_a	4
AlF_3/F^- inter-m. ligand exchange	water	–	–	$1.3 \cdot 10^{7}$	I_a	4
$Al(Cit)^{3-}$/Cit inter-m. ligand exchange	water	43 ± 1	−90 ± 29	1.0 ± 0.1	I_a	5
$Al_3(H_{-1}Cit)_3(OH)_4^{7-}$/Cit water assisted inter-m. ligand exchange	water	65 ± 7	−78 ± 21	0.08 ± 0.01	I_a	5
$Al_3(H_{-1}Cit)_3(OH)_4^{7-}$/intra-m. rearrangement	water	70 ± 5	34 ± 15	230	bond-rupture	5
$Al(acac)_2$ (hfac)/intramolecular rearrangement	CH_2Cl_2	(90)[a]	(+45)[a]	0.86	bond-rupture	6
$Al(acac)_3$/acac inter-m. ligand exchange	Hacac	85	−38	$9.1 \cdot 10^{-5}$	I_a	7
$Al(tfac)_3$/intra-m. site exchange	$CDCl_3$	114	+68	0.65 at 358K	bond-rupture	8

[a] Values in parentheses give Arrhenius activation energies.

1 (Hugi-Cleary et al., 1985); 2 (Phillips et al., 1997b); 3 (Phillips et al., 1997a); 4 (Bodor et al., 2000); 5 (Bodor et al., 2002a, 2002b); 6 (Case and Pinnavaia, 1971); 7 (Saito et al., 1990); 8 (Grossmann and Haworth, 1984).

tively fast racemization without any intermolecular oxalate exchange.

The qualitative pseudo-first-order rate constant values for intermolecular oxalate exchange reactions between the binary complexes, k_{12}, k_{13}, k_{24}, k_{24}, have similar magnitude (see Table 4) to $k_{30.}$ Based on this similarity one can consider the former also as real first-order constants. In other words, a D or I_d mechanism might be proposed for the ligand exchange between the complexes, also involving dissociation of an oxalate ligand from the complexes.

A closer inspection of the 2D EXSY spectra of the ternary system (shown in Fig. 8b) requires explanation of cross peaks between AlF_2^{+} and AlF_3. One has to note that a small quantity of HF/F^- exists, but it lies outside the measurement window. In the Al(III)–F^- system it is demonstrated that the formation reaction of AlF_3 from AlF_2^{+} and F (F means HF/F^-) is an unmeasurably slow process (Bodor et al., 2000). Therefore, this reaction cannot be responsible for these cross peaks. Direct F^- exchange between AlF_3 and AlF_2 is also ruled out. However, it can be shown that during the mixing time of 0.3 s the following chain of exchange reactions can produce magnetization transfer between the two binary complexes (i.e., follow the route of $^*F$):

$$Al^*FF^+ + F \rightleftharpoons AlF_2^+ + {}^*F \quad (8)$$

$$AlF_3 + {}^*F \rightleftharpoons Al^*FF_2 + F \quad (9)$$

Another interesting feature is that cross peaks are present between the complexes with different numbers of oxalate ligands in the inner coordination sphere, e.g., AlF_2Ox^- (4) and AlF_2^{+}, or AlF_2Ox^- (4) and $AlF_2Ox_2^{3-}$ (3). It would mean that intermolecular oxalate exchange, which is very slow in the binary oxalate complexes at room temperature, could be active for the ternary species. This would reflect the larger fluxionality of the $AlOx_2$ entity in $AlFOx_2^{2-}$and$AlF_2Ox_2^{3-}$ (see above). In fact, the F^- assisted indirect exchange via the following reactions (without any exchange of Ox) is a more plausible explanation:

$$Al^*FFOx^- + F \rightleftharpoons AlF_2Ox^- + {}^*F \quad (10)$$

$$AlF_2Ox_2^{3-} + {}^*F \rightleftharpoons Al^*FFOx_2^{3-} + F \quad (11)$$

However, no fluoride exchange was detected for $AlFOx_2$ (2). It resembles the inertness of AlF^{2+} to ligand exchange on the T_1 ^{19}F NMR time scale. This means that the single fluoride is not labile enough for detectable ligand exchange even in a complex where two bidentate oxalates are also coordinated to the Al(III). Moreover, in the Al(III)–pyrophosphate–F^- system the fluoride exchange reactions are much slower for higher complexes compared to our ternary system, allowing observation of spin-spin couplings between the ^{19}F nuclei. This might be attributed to the role of the multidentate pyrophosphate anion and/or its bridging position (Martinez et al., 1999).

It is also worth comparing these results to other Al(III)-organic ligand systems. The nonhydroxide assisted exchange of a citrate ligand (nonbridging $H_{-1}Cit^{4-}$, tridentate forming two six-membered chelate rings) of $Al_3(OH)_4(H_{-1}Cit)_3^{7-}$ with free citrate is faster and it has different activation parameters, $\Delta H^{\#}$ = 55 ± 7 kJ mol^{-1} and $\Delta S^{\#}$ = –78 ± 21 J mol^{-1} K^{-1}, supporting an $Al_3(OH)_4(H_{-1}Cit)_3,H_2O$ type transition state and I_a mechanism. The similar intermolecular exchange reaction of $Al(Cit)_2^{3-}$ (tridentate Cit^{3-}, forming one five-membered and one six-membered rings) is even faster, and an I_a mechanism can also be suggested (Bodor et al., 2002a). The difference in the mechanism and the definitely slower exchange of the five-membered AlOx entity (see Table 5) compared to the citrate in $Al(H_{-1}Cit)$ or Al(Cit) having two 6/6- or 6/5-membred rings (Bodor et al., 2002a) underline again the pronounced inertness of the chelating oxalate ligand in our studied system. The kinetic behavior of oxalate can vary substantially in other metal complexes. For example, the intermolecular oxalate exchange

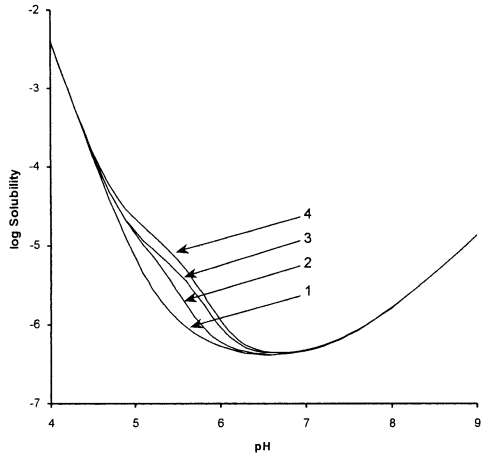

Fig. 9. Solubility of Gibbsite in the absence (1) and presence of ligands: (2) (c_{Ox} = 10 μM, c_F = 0 μM), (3) (c_{Ox} = 0 μM, c_F = 10 μM), (4) (c_{Ox} = 10 μM, c_F = 10 μM).

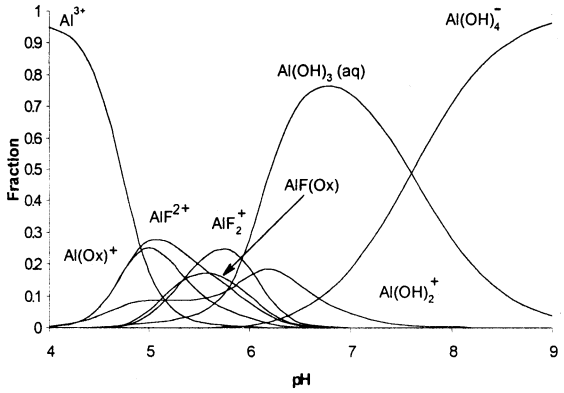

Fig. 10. Distribution diagram showing only the species in solution in equilibrium with Gibbsite in the presence of c_{Ox} = c_F = 10 μM.

reaction of the binary $UO_2(Ox_2)(H_2O)^{2-}$ complex with pentagonal bipyramid geometry has a second-order rate constant and negative activation entropy ($\Delta S^{\#}$ = –56 $Jmol^{-1}K^{-1}$), suggesting an I_a mechanism (Aas et al., 1999). Furthermore, the similar oxalate exchange reaction of the saturated ternary $UO_2(Ox)F_3^{2-}$ complex has a first-order rate constant and positive activation entropy ($\Delta S^{\#}$ = 23 J mol^{-1} K^{-1}), indicating a dissociative mechanism (Szabó and Grenthe, 1998).

4.3. Model Calculations

The values of the overall stability constants of the mixed Al(III)–Ox^{2-}–F^- complexes indicate that these species are surprisingly stable. For example, log$K(AlOx^+ + F^- = AlFOx)$ = 5.56. This value is less than one magnitude smaller than logK_1 (6.42) for the binary AlF^{2+} complex. Furthermore, log$K(Al(Ox)_2^- + F^- = Al\,F\,(Ox)_2^{2-})$ = 4.81, which indicates strong interactions between these two anions. The formation constant for the coordination of a second fluoride ion to $AlF(Ox)_n^{(3-2n-1)+}$ is 4.14 (n = 1) and 3.46 (n = 2). These values are also quite high in comparison with logK_2 = 5.4 for AlF_2^+. It can be concluded that the presence of one or two oxalate ions in the coordination sphere of Al(III) does not influence the affinity for fluoride ions too much. This is not a unique feature as similar observations are made in, for example, the aluminum(III)–EDTA–fluoride system (Nemes et al., 1998; Yuchi et al., 1996; Martin, 1996). All these findings emphasize the special strength of the aluminum(III)–fluoride interaction, indicating small changes of the effective charge of the aluminium ion as water molecules are replaced by O-containing ligands.

To demonstrate the significance of mixed Al(III)-Ox^{2-}-F^- complexes under conditions typical of natural waters, some model calculations have been performed. The computer code SOLGASWATER (Eriksson, 1979) was used with a chemical model presented in Table 2. In these calculations, gibbsite (α-$Al(OH)_3$) was allowed to be the Al-regulating solid phase. Furthermore, the total concentrations of oxalate and fluoride were set to 10^{-5} M, which are concentration levels typical of natural waters (Graustein et al., 1977; Stumm and Morgan, 1996). It is clear from the solubility curves presented in Figure 9 that an increase in the solubility of gibbsite due to Al-complexation to these ligands is obtained within the pH range 4.5–6.5. The maximum increase is approximately 10-fold in the presence of both ligands (see curve 4) at pH $\approx$ 5.5, a pH value typical of many surface waters. From the distribution diagram shown in Figure 10 it can be seen that some 20% of total Al in solution is in the form of AlFOx. It may thus be concluded that mixed Al(III)–Ox^{2-}–F^- complexes have to be considered as the chemical speciation of Al(III) in natural waters is discussed.

All constants have been determined at an ionic strength of 0.6 mol/L, except for those marked with an asterisk. Those have been extrapolated from zero ionic strength using the ionic strength dependence given by Baes and Mesmer for the binary Al(III)-OH^- complexes. They found the equation, $\log Q_{xy} = \log K_{xy} + aI^{1/2}/(1+ I^{1/2}) + bI$, to adequately describe a great number of hydrolysis reactions within wide ranges in ionic strength. Here K_{xy} denotes the constant at infinite dilution (I = 0) and a = 0.51 Δz^2. Δz^2 is the square of the charge of each species summed over the formation reaction. b is regarded as a parameter reflecting short-range nonelectrostatic interactions at high I including also the effect of the water activity on Q_{xy}. In the extrapolations, species of the same charge have been assumed to have the same value of the b parameter of the expression above.

Acknowledgments—We thank Professor I. Grenthe (KTH, Stockholm) for supervising A.B. in potentiometric study and for valuable discussions and one of the anonymous referees for valuable suggestions in chemistry and grammar. The authors are grateful to the Hungarian Science Research Foundation (OTKA), Project T 026115 and T 038296 and the Swedish Natural Research Council for financial support.

Associate editor: W. H. Casey

REFERENCES

Aas W., Szabó Z., and Grenthe I. (1999) Equilibria and dynamics in binary and ternary uranyl oxalate and acetate/fluoride complexes. *J. Chem. Soc., Dalton Trans.* 1311–1317.

Baes C. F. and Mesmer R. E. (1976) *The Hydrolysis of Cations*. John Wiley & Sons, Inc.

Bányai I., Glaser J., and Tóth I. (2001) Cyanide exchange on $Tl(CN)_4^-$ in aqueous solution studied by ^{205}Tl and ^{13}C NMR. *Eur. J. Inorg. Chem.* 1709–1717.

Bodor A., Tóth I., Bányai I., Szabó Z., Zékány L., and Hefter G. T. (2000) ^{19}F-NMR study of equilibria and dynamics of the Al^{3+}/F^- system. *Inorg. Chem.* **39,** 2530–2737.

Bodor A., Bányai I., Zékány L., and Tóth I. (2002a) Slow dynamics of aluminum–citrate complexes studied by ^1H and ^{13}C NMR spectroscopy. *Coord. Chem. Rev.* **228,** 163–173.

Bodor A., Bńyai I., and Tóth I. (2002b) ^1H and ^{13}C NMR as tools to study aluminum coordination chemistry–aqueous Al(III)–citrate complexes. *Coord. Chem. Rev.* **228,** 175–186.

Brosset C. and Orring J. (1943) Studies of the consecutive complex formation of aluminum fluoride complexes. *Svensk. Kem. Tidskr.* **5,** 101–116.

Case D. A. and Pinnavaia T. (1971) Kinetics of stereochemical rearrangements for mixed β-diketonate complexes of aluminum(III). *Inorg. Chem.* **10,** 482–486.

Casey W. H. and Westrich H. R. (1992) Control of dissolution rates of orthosilicate minerals by divalent metal-oxygen bonds. *Nature* **355,** 157–159.

Chan S. O. and Reeves L. W. (1970) Nuclear magnetic resonance studies of multi-site chemical exchange. I. Matrix formulation of the Bloch equations. *Can. J. Chem.* **48,** 3641–3653.

Ehde P. M., Pettersson L., and Glaser J. (1991) Multicomponent polyanions. 45: A multinuclear NMR study of vanadate(V)-oxalate complexes in aqueous solution. *Acta Chem. Scand.* **45,** 998–1005.

Eriksson G. (1979) An algorithm for the computation of aqueous multi-component, multiphase equilibria. *Anal. Chim. Acta* **112,** 375–383.

Gran G. (1952) Determination of equivalence point in potentiometric titrations. Part II. *Analyst* **77,** 661–667.

Graustein W. C., Cromack K., and Sollins P. (1977) Calcium-oxalate-occurrence in soils and effect on nutrient and geochemical cycles. *Science* **198,** 1252–1254.

Grossmann D. L. and Haworth D. T. (1984) A dynamic ^1H–NMR study of Tris(trifluoro-2,4-pentanedionato) chelates of aluminum(III) and gallium(III). *Inorg. Chim. Acta* **84,** L17–19.

Hefter G. T., Bodor A., and Tóth I. (2000) Does AlF_6^{3-} exist in solution? *Austr. J. Chem.* **53,** 625–626.

Hugi-Cleary D., Helm L., and Merbach A. E. (1985) Variable temperature and variable pressure ^{17}O NMR study of water exchange of hexaaquaaluminum(III). *Helv. Chim. Acta* **68,** 545–554.

Irving H. M., Miles M. G., and Pettit L. P. (1967) A study of some problems in determining the stoichiometric proton dissociation constants of complexes by potentiometric titrations using a glass electrode. *Anal. Chim. Acta* **38,** 475–488.

Jaber M., Bertin F., and Thomas-David G. (1977) Application de la spectrometrie infrarouge, Raman et resonance magnetique nucleaire a l'etude des complexes en solution aqueuse, Al^{3+}-$H_2C_2O_4$. *Can. J. Chem.* **55,** 3689–3699.

Long F. A. (1941) The exchange of oxalates of some complex trioxalate ions of trivalent metals. *J. Am. Chem. Soc.* **63,** 1353–1357.

Martin R. B. (1996) Ternary complexes of Al^{3+} and F^- with a third ligand. *Coord. Chem. Rev.* **149,** 23–32.

Martinez E. J., Girardet J.-L., Maerschalk C., and Morat C. (1999) Determination by multi-NMR studies of new stable aluminum complexes with pyrophosphate and fluoride in aqueous solution. *Inorg. Chem.* **38,** 4765–4770.

Mörtl K. P., Sutter J.-P., Golhen S., Ouahab L., and Kahn O. (2000) Structure and magnetic characteristics of an oxalate-bridged U(IV)–Mn(II) three-dimensional network. *Inorg. Chem.* **39,** 1626–1627.

Nemes J., Tóth I., and Zékány L. (1998) Formation kinetics of an aluminium(III)-ethylenediamine-tetraacetate-fluoride mixed ligand complex. *Chem. Soc., Dalton Trans.* 2707–2713.

Orrell K. G., Šik V., and Stephenson D. (1990) Quantitative investigation of molecular stereodynamics by 1D and 2D NMR methods. *Prog. NMR Spectr.* **22,** 141–208.

Phillips B. L., Casey W. H., and Crawford S. N. (1997a) Solvent exchange in $AlF_x(H_2O)_{6-x}^{3-x}$(aq) complexes: Ligand-directed labilization of water as an analogue for ligand-induced dissolution of oxide minerals. *Geochim. Cosmochim. Acta* **61,** 3041–3049.

Phillips B. L., Crawford S. N., and Casey W. H. (1997b) Rate of water exchange between $Al(C_2O_4)(H_2O)_4^+$(aq) complexes and aqueous solutions determined by ^{17}O-NMR spectroscopy. *Geochim. Cosmochim. Acta* **61,** 4965–4973.

Powell A. K. and Heath S. L. (1996) X-ray structural analysis of biologically relevant aluminum(III) complexes. *Coord. Chem. Rev.* **149,** 59–80.

Puigdomenech I (1997) *MEDUSA* (Windows Interface to the MS-DOS Version of INPUT, SED and PREDOM Fortran Program Drawing Chemical Equilibrium Diagrams). Program is available at http://www.inorg.kth.se/MEDUSA/.

Saito K., Kido H., and Nagasawa A. (1990) Reactivity and reaction mechanism of acetylacetonato complexes of tervalent metal ions in solution. *Coord. Chem. Rev.* **100,** 427–452.

Sandström J. (1982) *Dynamic NMR Spectroscopy*. Academic Press, London, p. 17.

Sanjuan B. and Michard G. (1987) Aluminum hydroxide solubility in aqueous solution containing fluoride ions at 50°C. *Geochim. Cosmochim. Acta* **51,** 1823–1832.

Sillén L. G. and Warnquist B. (1968) High-speed computers as supplement to graphical methods. 8. *Arkiv Kemi.* **31,** 365–376.

Sjöberg S. and Öhman L.-O. (1985) Equilibrium and structural studies of silicon(IV) and aluminium(III) in aqueous solution. Part 13: A potentiometric and ^{27}Al nuclear magnetic resonance study of speciation and equilibria in the aluminium(III)–oxalic acid-hydroxid system. *J. Chem. Soc., Dalton Trans.* 2665–2669.

Smith R. W. (1996) Kinetic aspects of aqueous aluminum chemistry: Environmental implications. *Coord. Chem. Rev.* **149,** 81–94.

Stumm W. and Morgan J. J. (1996) *Aquatic Chemistry*. 3rd ed. John Wiley & Sons, Inc.

Szabó Z. and Grenthe I. (1998) Mechanisms of ligand substitution reactions in ternary dioxouranium(VI) complexes. *Inorg. Chem.* **37,** 6214–6222.

Taube H. (1952) Rates and mechanisms of substitution in inorganic complexes in solution. *Chem. Rev.* **50,** 69–126.

van Geet L. A. (1970) Calibration of methanol nuclear magnetic resonance thermometer at low temperature. *Anal. Chem.* **42,** 679–680.

Yuchi A., Hokari N., Terao H., and Wada H. (1996) Complexes of hard metal ions with amine-*N*-polycarboxylates as fluoride receptors. *Bull. Chem. Soc. Jpn.* **69,** 3173–3177.